Chem Soc Rev

Chemical Society Reviews

www.rsc.org/chemsocrev

Volume 37 | Number 2 | February 2008 | Pages 237–432

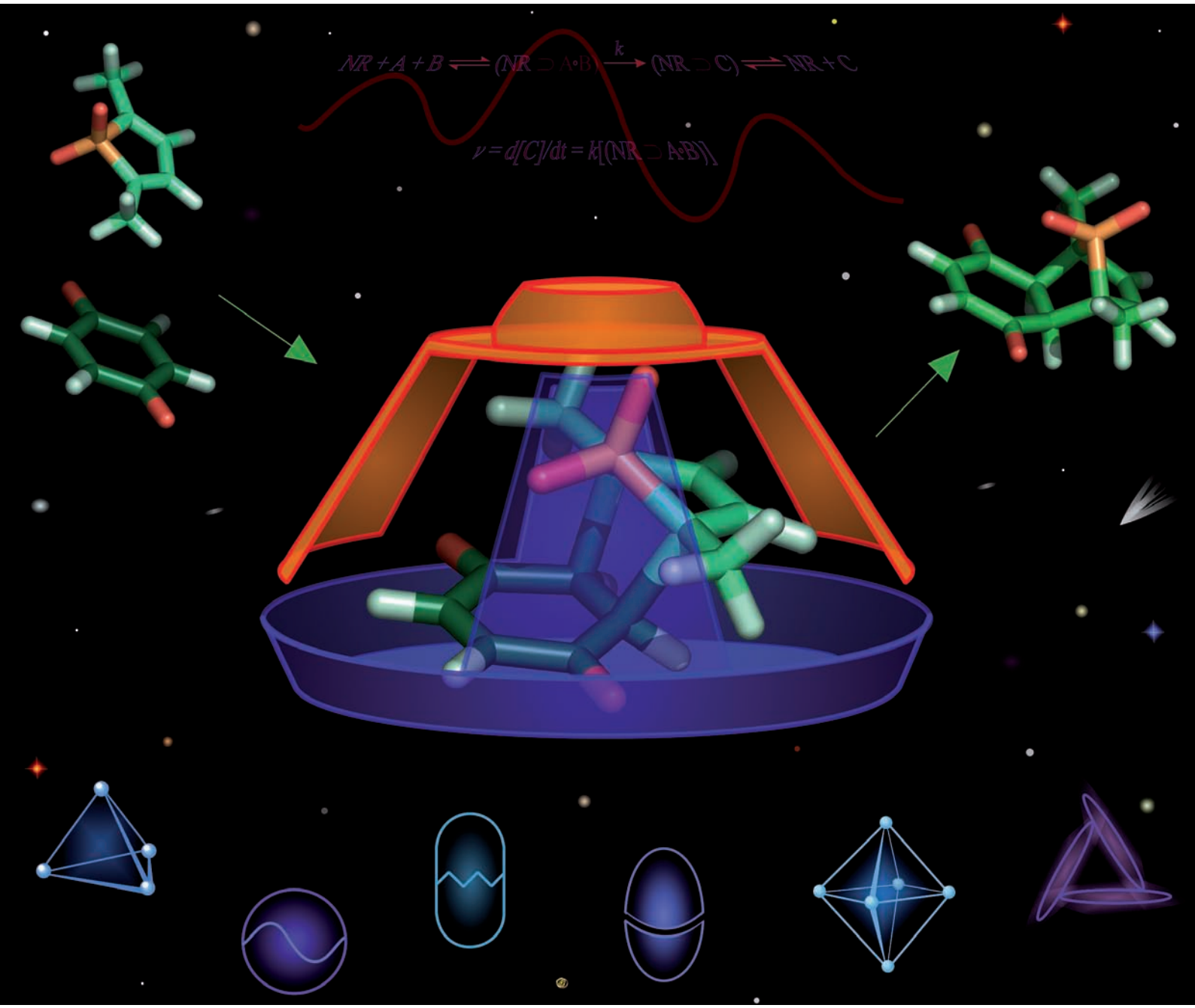

ISSN 0306-0012

RSC Publishing

Reactivity within a confined self-assembled nanospace

Tehila S. Koblenz, Jeroen Wassenaar and Joost N. H. Reek*

Received 28th September 2007
First published as an Advance Article on the web 19th October 2007
DOI: 10.1039/b614961h

Confined nanospaces in which reactions can take place, have been created by various approaches such as molecular capsules, zeolites and micelles. In this *tutorial review* we focus on the application of self-assembled nanocapsules with well-defined cavities as nanoreactors for organic and metal catalysed transformations. The self-assembly of nanocapsules based on noncovalent bonds such as hydrogen bonds and metal–ligand interactions is discussed to introduce the properties of the building blocks and capsules thereof. We will elaborate on the encapsulation effects that can be expected when reactions are carried out in a capsule-protected environment. Subsequently, literature examples will be described in which self-assembled nanocapsules are applied as nanoreactors, for various types of organic and metal catalysed reactions.

1. Introduction

The worldwide increase in population and the ever increasing standard of living puts enormous demands on the resources of the planet and in order to keep (or get) the human population in balance with the environment we should completely turn to sustainable processes. This implies that many synthesis routes currently used for bulk chemicals, pharmaceutical and chemical intermediates should be replaced by more efficient methods starting from renewable resources. Looking at the current state of affairs, we can conclude that there is still a long way to go. Evidently catalysts, substances that promote, accelerate and control chemical reactions, are indispensable to arrive at sustainable processes and a tremendous progress in transition metal catalysis, organocatalysis and enzyme catalysis has been made in the past decades.[1–3] From the progress made in synthesis and catalysis so far we also learn that there is an urgent need for more tools and deeper understanding.

Supramolecular and Homogeneous Catalysis, van't Hoff Institute for Molecular Sciences, University of Amsterdam, Nieuwe Achtergracht 166, Amsterdam, 1018 WV, The Netherlands.
E-mail: reek@science.uva.nl; Fax: +31 20 5255604; Tel: +31 20 5256437

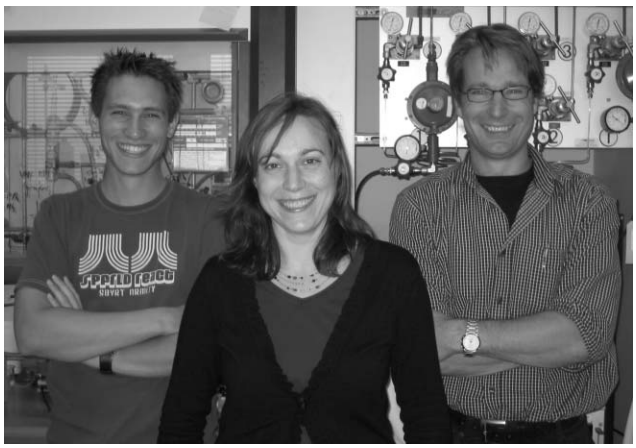

Jeroen Wassenaar Tehila S. Koblenz Joost N. H. Reek

Tehila Koblenz was born in Amsterdam, the Netherlands in 1977. She obtained her MSc degree in Chemistry (cum laude) from the University of Amsterdam in 2003. As an undergraduate student, she worked on organometallic chemistry and on homogeneous transition metal catalysis in the laboratories of Prof. C. J. Elsevier at the same university and of Prof. D. Milstein at The Weizmann Institute of Science in Israel. Currently, she is working on her PhD degree at the University of Amsterdam under the guidance of Prof. J. N. H. Reek and Prof. P. W. N. M. van Leeuwen. Her research includes supramolecular chemistry and homogeneous transition metal catalysis.

Jeroen Wassenaar was born in Munich, Germany, in 1983. He obtained his MSc degree in Chemistry (cum laude) from the University of Amsterdam in 2006. As a undergraduate student he worked on homogeneous transition metal catalysis and supramolecular chemistry in the laboratories of Prof. C. J. Elsevier and Prof. J. N. H. Reek at the same university and Prof. K. B. Sharpless at The Scripps Research Institute in California. Currently, he is working on his PhD degree at the University of Amsterdam under the guidance of Prof. J. N. H. Reek. His research focuses on asymmetric catalysis and dynamic combinatorial chemistry.

Prof. Dr Joost Reek (1967) did his masters at the University of Nijmegen and finished his PhD in the area of supramolecular chemistry in the group of Prof. R. J. M. Nolte in 1996 at the same university. He joined the group of Prof. M. J. Crossley in Sydney as a postdoctoral fellow in 1996, where he, among other things, gained experience in porphyrin chemistry. In January 1998 he became lecturer (senior lecturer in 2003) in the group of Prof. P. W. N. M. van Leeuwen at the University of Amsterdam with research activities focusing on transition metal catalysis, dendritic catalysis and catalyst recovery. In 2005 he became a young member of royal Dutch academy of sciences (KNAW) and in 2006 he was appointed full professor (chair supramolecular catalysis) at the University of Amsterdam. His current research interests include transition metal catalysis, supramolecular chemistry, supramolecular catalysis, catalyst immobilization and dendritic transition metal catalysis.

Enzymes, nature's creation of catalysts, encapsulate multiple functionalities within their cavity where the catalytic conversion takes place, and can be extremely active and selective for a range of chemical conversions. Therefore, enzymes have served as the major source of inspiration for supramolecular catalysis, but at the same time the working principles of enzymes are still subject to debate. Already in 1948 Pauling proposed that enzymes stabilize transition states to a larger extent than reagents in their (vibrational) ground state by means of noncovalent interactions between the functional groups in the enzyme cavity and the compounds inside the cavity.[4] These initial ideas, that are still valid to a large extent, have inspired many scientist from various fields to explore similar approaches for synthetic systems. The main focus in the area of supramolecular catalysis has been on host–guest catalysis in which a substrate is bound in a cavity next to the catalytically active centre. The general approach applied was combining known catalysts and functional groups near the catalytic centre that function as the binding site by recognizing the substrate by noncovalent interactions. This approach has resulted in numerous interesting examples of supramolecular catalysts.[5] However, these catalysts do not even come close to the catalyst efficiency and selectivity displayed by enzymes.

Enzymes are much more than just a combination of a substrate binding site and a catalytically active site. Indeed it has been demonstrated that many other effects play an important role, including substrate preorganization, restricted substrate motion, protein dynamics, covalent binding of the transition state and desolvation of the substrate.[6] The special microenvironment within the enzyme cavity induces most of these effects. Generally, the reaction medium is known to greatly affect chemical reactions. If a reaction takes place in the enzyme cavity, the reactants and the transition state are stripped from solvent molecules which are replaced by the microenvironment created around the substrates. This implies some precisely placed interactions and a different dielectric constant. Interestingly, these cavity effects are difficult to study and have been mainly proposed on the basis of computational studies. A tool to create nanosized reaction chambers, *i.e.* nanoreactors, is therefore very interesting, since it enables these effects to be studied experimentally with synthetic analogues. In addition, the ability to control the reaction environment by creating a confined and well-defined nanospace around the substrates can provide new tools to develop future sustainable catalytic processes.

Molecular capsules have hollow structures and encapsulate smaller guest molecules within their cavities. Since the nineties of the last century, research groups around the world have investigated the application of nanocapsules as nanoreactors, *i.e.* reaction vessels for chemical transformations, and have used the nanocapsules for studying the different cavity effects.[7,8] Besides molecular capsules also other assemblies such as micelles and vesicles have been applied as nanoreactors, but these systems are beyond the current scope of the review.[7] In this review we will focus on the application of self-assembled nanocapsules as nanoreactors. In section 2 different types of nanocapsules are discussed: capsules based on hydrogen bonds, metal–ligand interactions and hydrophobic effects. In section 3 nanocapsules that encapsulate an active-site are discussed. Section 4 discusses the effects that can be expected if reactions are carried out in nanocapsules, and in section 5 we will provide examples that support these views.

2. Self-assembled nanocapsules

Supramolecular chemistry, defined by Jean-Marie Lehn as the 'chemistry beyond the molecule', is the application of programmed molecules that assemble into larger molecular architectures *via* intermolecular noncovalent bonds.[9,10] An important class of supramolecular structures are the host–guest assemblies, where the host is a receptor that selectively binds (generally smaller) guest molecules.[11–13] Initial focus in the area of supramolecular chemistry was strongly on development of host–guest systems such as cyclodextrins, calixarenes, clefts, and clip shaped receptors. This was important to gain fundamental knowledge on noncovalent interactions between molecules and it also formed the basis for sensor applications and further development of larger systems. Host molecules can have open or closed cavities to accommodate the guest molecule and the guest is at least partly stripped from the solvent. Cyclodextrins and cucurbiturils are important examples of host molecules with open cavities.

Molecular capsules are a special class of host molecules with an important three-dimensional structure. Binding within molecular capsules occurs by complete encapsulation of the guest within the enclosed internal space, *i.e.* the cavity.[14] Two types of these nanometer sized molecular capsules can be distinguished; the capsules based on covalent bonds and those based on noncovalent interactions, *i.e.* self-assembled or supramolecular capsules.† Initial research in this area was on covalent capsules such as hemicarcerands, and calixarenes- and CTV (cyclotriveratrylene) based capsules. Guest exchange in-and-out of noncovalent capsules can, in addition to the gating mechanism, proceed *via* (partial) dissociation of the capsule (*vide infra*). Consequently, guest exchange is often, but not always, more facile for noncovalent capsules compared to their covalent counterparts. Another advantage of noncovalent capsules can be the circumvention of tedious multistep synthesis which is necessary for the formation of covalent capsules. In this review we will focus on the chemistry taking place inside self-assembled capsules with closed cavities. However, one should keep in mind that the boundaries between capsules with open- and closed cavities are not always very clear.

Self-assembled capsules are composed of two or more, not necessarily identical, building blocks programmed to self-assemble in solution into the desired supramolecular capsule. The self-assembly process is primarily driven by the formation of multiple intermolecular noncovalent bonds such as hydrogen-bonds, metal–ligand- and ionic interactions between the building blocks. Therefore the capsule's building blocks are functionalized with complementary binding motifs. The reversible and directional nature of the noncovalent bonds facilitate self-control and self-correction, which results in the

† In the early days of this research field capsules based on covalent bonds were also assigned as 'supramolecular capsules' because of their encapsulation properties. However, because of the developments of the last decade we designate here only capsules based on covalent interactions as 'supramolecular capsules'.

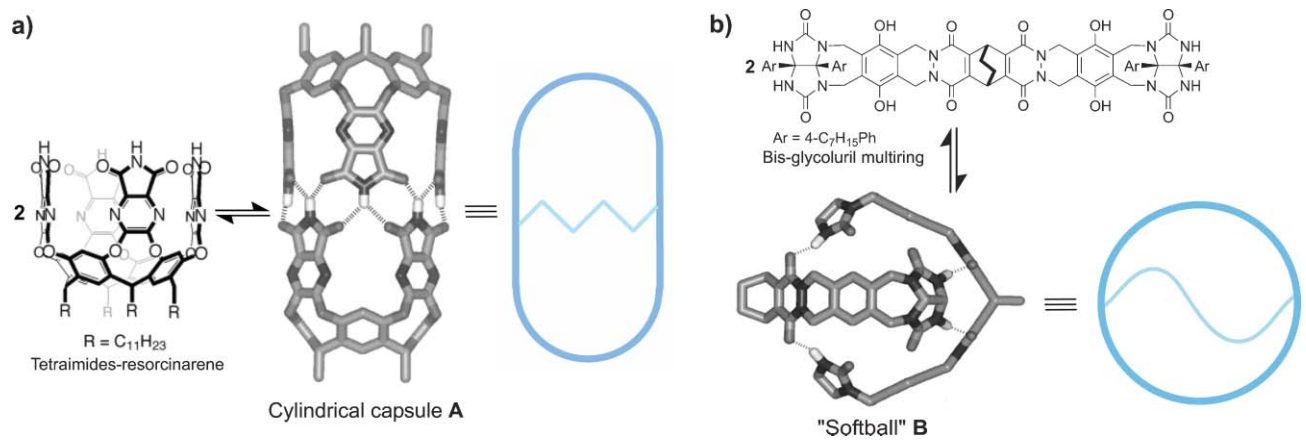

Fig. 1 a) Cylindrical capsule **A**. b) ''Softball'' capsule **B**. In the modeled structures some substituents, hydrogen atoms and hydrogen bonds have been omitted for clarity. Reproduced in part with permission from Wiley InterScience from reference 17.

formation of a discrete thermodynamically stable capsule.‡ Complementarity of size and shape between the building blocks is necessary for a successful self-assembly and the formation of a proper capsular structure. The correct capsular structure (especially of H-bonded capsules) is often achieved by employing curvature containing building blocks such as the concave calix[4]arene. In most examples the presence of appropriate guest molecules during the assembly process are necessary for templating the assembly of a specific capsule.

Selective guest recognition and reversible encapsulation form the essential properties of self-assembled capsules. The guests can be organic- or organometallic compounds. Guest encapsulation can be thermodynamically or entropically driven. The latter is generally observed when more (solvent) molecules are released upon guest encapsulation. Molecular recognition and guest encapsulation depend on size, shape and chemical-surface complementarities between the guest molecule(s) and the capsule's cavity. In addition, noncompetitive solvents that do not (or poorly) fit inside the capsule's cavity, favour the encapsulation of external guests. Guest encapsulation is generally reversible and the guest(s) can enter and exit the host *via* different pathways, depending on the capsule's properties (*vide infra*). Guest orientation and motion within the capsule's cavity are restricted and depend on shape complementarity, steric hindrance and noncovalent interactions such as CH–π interactions and π–π stacking between the guest and host. The hydrophobic environment inside the capsule can assist guest encapsulation or orientation. The aromatic rings of the nanocapsules cause anisotropic shielding of the guest, enabling guest detection by proton NMR techniques. Upon encapsulation the guest molecules are temporarily isolated from the bulk and experience a novel finite microenvironment, which can change reaction pathways. Encapsulation of a single guest or simultaneously encapsulation of two or more guests have promoted uni- and bimolecular reactions within the capsules as is discussed in sections 4 and 5.

‡ It is also possible to isolate kinetically formed capsules, however the practical value of these structures remains to be seen since they probably rearrange or decompose upon use.

2.1 Capsules based on hydrogen bonds

The weak, highly directional, and dynamic nature of hydrogen bonds makes them very suitable as a noncovalent interaction for the formation of supramolecular capsules. Hydrogen bonded capsules are formed instantly upon solvation of their building blocks and their dissociation and recombination is generally more dynamic than that of the metal–ligand based capsules. The lifetime of the different H-bonded capsules range from microseconds to hours, depending for example on the number of hydrogen bonds formed upon capsule formation.[15–17] Capsule assembly is induced by guest encapsulation which can be solvent molecules or specific guests. Rebek and co-workers have shown that optimal guest occupation is *ca.* 55% of the available volume of the cavity. However, stable self-assembled capsules with guests that occupy much more or less than 55% also exist. Most H-bonded capsules do not have sizeable apertures for guest exchange and consequently guest exchange occurs *via* partial or complete rupture of the capsule, depending on the properties of the host, guest and solvent. The residence time of the guest within the capsule is in the order of milliseconds to hours. H-bonded capsules are stable in apolar organic solvents such as dichloromethane and mesitylene while competitive solvents like DMSO and water cause capsule dissociation.

Rebek and co-workers have developed the cylinder-shaped capsule **A**.[15–17] This capsule consists of two self-complementary vase-shaped cavitands, *i.e.* resorcinarenes, substituted with four imide-functionalities on their upper rim (Fig. 1a). The cavitands dimerize in solution into the cylindrical capsule **A** upon the formation of a seam of eight bifurcated hydrogen bonds (*i.e.* sixteen H-bonds). Capsule **A** has a cylindrical cavity with an internal volume of *ca.* 425 $Å^3$. The cavity contains a gradient of polarity and shape along its length and accommodates elongated guests. The capsule can simultaneously encapsulate two different guests, *i.e.* selective pairwise recognition, such as one molecule of benzene together with one *p*-xylene molecule, which can be of interest for coupling reactions. During guest exchange two flaps of the capsule open, allowing guest exchange without capsule dissociation.

The ''softball'' capsule **B**, also developed by Rebek and co-workers, is composed of two multiring structures having a

bridged bicyclic centrepiece and two glycoluril units on both ends of the multiring, providing the proper rigidity, curvature and functional groups necessary for capsule assembly (Fig. 1b).[15–17] The self-complementary glycoluril-based building blocks dimerize in solution into capsule **B** upon the formation of a seam of sixteen hydrogen bonds. "Softball" **B** is a closed-shell capsule of roughly spherical shape with an internal volume of *ca.* 400 $Å^3$. The "softball" can simultaneously encapsulate two different guests such as one molecule of deuterated benzene together with one molecule of deuterated monofluorobenezene. Guests encapsulation occurs by opening of two separate flaps of the "softball" and subsequently departure of the guest as the incoming guest approaches, *i.e.* gating mechanism.

2.2 Capsules based on metal–ligand interactions

Metal–ligand interactions are strong and highly directional and lead to the self-assembly of robust stable coordination cages.[18] Kinetically labile metal–ligand (M-L) interactions are essential for converting initially formed kinetic products to the more stable thermodynamic product. Therefore appropriate conditions should be applied for the assembly of M-L based capsules in high yields. The metal coordination geometry in combination with multidentate organic ligands are used as codons for curvature. The preorganized and rigid nature of the ligands results in stable and well defined capsules with cage-like architectures. Unlike H-bonded capsules, guest exchange in and out of the coordination cages occurs by expansion of the cage apertures without M-L bond rupture.[19] Consequently, the size and shape of the cage apertures function as a gate keeper as they dictate the permitted size and shape of the guests.

Raymond and co-workers have developed the chiral tetrahedral $[M_4L_6]^{12-}$ coordination cage **C** consisting of four metal ions with an octahedral coordination geometry, *e.g.* Ga^{3+}, and six naphthalene-based bis-bidentate catechol amide ligands (Fig. 2a).[20] The metal ions are situated at the corners of the tetrahedron and the ligands span the edges of the tetrahedron. The tris-bidentate chelation of the metal atoms renders them chiral (Δ or Λ), and the mechanical coupling between the metals through the rigid ligands results in the exclusive formation of the homochiral assemblies Δ,Δ,Δ,Δ and Λ,Λ,Λ,Λ. The desired M_4L_6 stoichiometry with a tetrahedral shaped cage is achieved by the presence of an appropriate guest template during the assembly process such as NR_4^+ (R = Me, Et, Pr). The negatively charged tetrahedral cage is soluble in water and other polar solvents and contains a hydrophobic cavity of 300–500 $Å^3$. The highly anionic character of the cage allows for exclusive encapsulation of monocationic guests such as alkylammonium ions and cationic organometallic complexes such as $[CpRu(C_6H_6)]^+$ (Cp = η^5-C_5H_5).

Fujita and co-workers have designed the octahedral $[M_6L_4]^{12+}$ coordination cage **D** composed of six *cis*-protected square planar Pd^{2+} or Pt^{2+} complexes, *e.g.* $[Pd(en)]^{2+}$, and four panel-like ligands, *i.e.* the triangular tridentate 2,4,6-tris(4-pyridyl)-1,3,5-triazine ligand (Fig. 2b).[21,22] The metal complexes are situated at the corners of the octahedron and the ligands alternatively occupy the eight faces of the octahedron. The positively charged octahedral cage is soluble in water and contains a hydrophobic environment. Consequently, this cage can strongly bind a variety of anionic and neutral guest molecules such as adamantine and ferrocene. Guest exchange can take place *via* the relatively large pores of the host. The large inner cavity has a diameter of *ca.* 2.2 nm and allows encapsulation of one to four guest molecules per cage, depending on the guest size. The coordination cage **D** can pairwise selectively recognize two different guests such as one anthracene-type molecule and one maleimide-type molecule. Remarkably, no external guests are needed in order to selectively form the Pd-based octahedral cage and the cage can be prepared at large scale (up to 50 g). This indicates that also polar solvents such as water can be in the cage. The Fujita group has reported many other cage type structures, but cage **D** has been mostly used as reaction vessel.

2.3 Capsules based on hydrophobic effects

Gibb and co-workers have explored water-soluble cavitands that self-assemble into capsule **E**. The assembly process is based on hydrophobic effects (and possibly on non-directional π–π stacking between the two building blocks) and the capsule

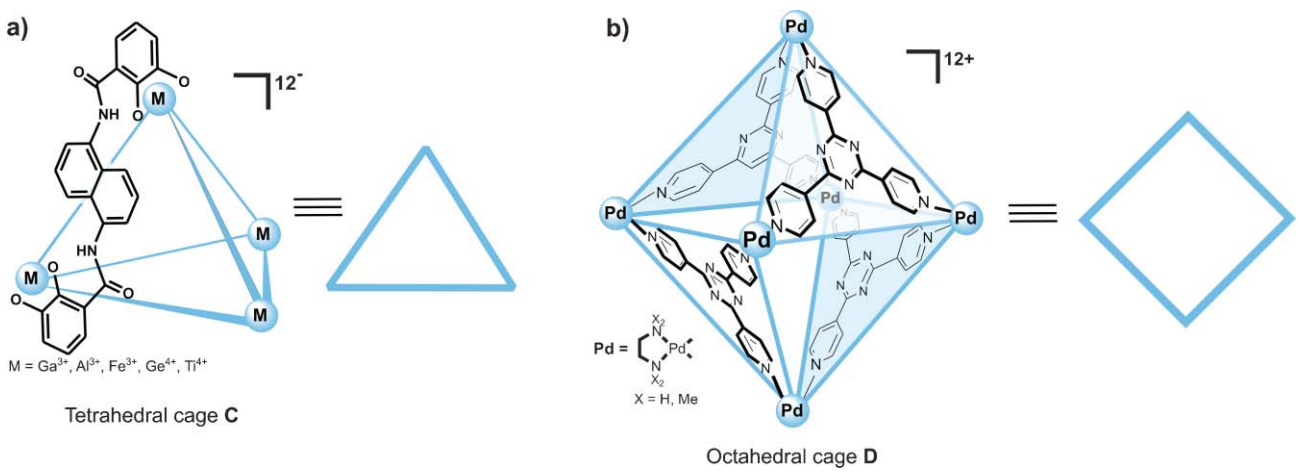

Fig. 2 a) Tetrahedral M_4L_6 coordination cage **C**. b) Octahedral M_6L_4 coordination cage **D**.

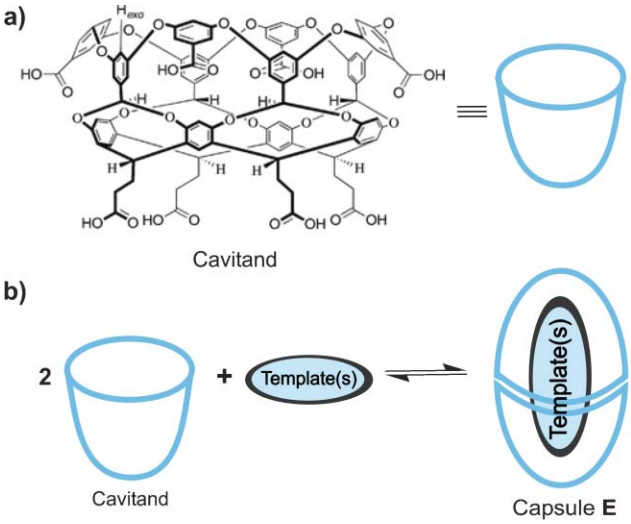

Fig. 3 a) Deep-cavity cavitand. b) Self-assembly of capsule **E**.

formation occurs only in the presence of hydrophobic guests that function as template.[23] The template plays an important role in the formation of capsule **E** because no directional noncovalent bonds such as H-bonding and M-L interactions are involved in the self-assembly process. In addition, an external hydrophobic template is necessary because the aqueous solvent does not template the formation of **E**. However, one should not forget that the presence of an appropriate template (other than solvent) is necessary for the formation of most self-assembled capsules. Capsule **E** consists of two octa-acid, deep-cavity cavitands with a pseudo-conical hydrophobic cavity (Fig. 3a). The eight carboxylic acid groups are located at the periphery of the cavitand and engender water-solubility under basic conditions. The cavitands dimerize upon encapsulation of complementary hydrophobic templates such as a rigid steroid or two smaller alkanes (Fig. 3b). As is mentioned above, the capsule is also held together by non-directional π–π stacking between the aromatic rings on the wide hydrophobic rim of the two cavitands and therefore the structural integrity of these capsules is not fixed. Capsule **E** has a capsular form with an internal cavity of *ca.* 500 Å^3.

3. Active-site encapsulation

Most reactions do not occur spontaneously and require the presence of a catalyst, which can be a Lewis acid site or a transition metal to activate certain bonds (for example C–Br or C–H bonds). Besides the encapsulation of substrate molecules to facilitate certain conversions, also the active centre can be encapsulated. Indeed sufficient space should be available to allow the transformation of encapsulated substrates at the active site.

Raymond and co-workers have encapsulated cationic transition metal complexes such as $[Cp^*(PMe_3)Ir(Me)(C_2H_4)]^+$ and $[(PMe_3)_2Rh(COD)]^+$ within their tetrahedral coordination cage **C** *via* non-directional noncovalent bonds (Fig. 4). These encapsulated active-sites were successfully used for C–H bond activation and isomerization reactions (*vide infra*).[24,25]

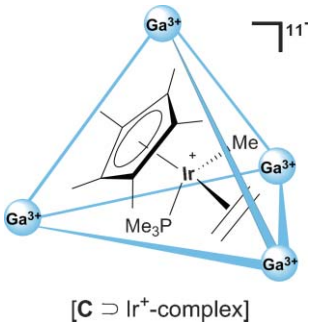

Fig. 4 Cationic Ir-complex encapsulated within **C**, *i.e.* [**C** ⊃ Ir^+-complex] (this notation denotes that **C** encapsulates an Ir^+-complex).

Active-site encapsulation can also be achieved by directional noncovalent bonds such as metal–ligand interactions. Hupp and co-workers have described the assembly of an open box structure **F** encapsulating a Mn^{III}-porphyrin *via* metal–ligand interactions.[26] The open box **F** is based on four Zn^{II}-porphyrins coordinated to four $[Re(CO)_3Cl]$ complexes *via* their pyridyl ligands. The encapsulated Mn^{III}-porphyrin appeared to be a stable and selective epoxidation catalyst. Although the open box type assemblies are beyond the scope of this review, it is important to realize that these more open assemblies can also provide interesting catalysts.

Reek and co-workers have introduced the ligand–template approach as a new strategy for the encapsulation of transition metal catalysts.[27–31] The template ligands have a bifunctional character in that they contain functional groups for capsule assembly as well as a donor-atom site for metal coordination. This results in the encapsulation of the metal within the ligand–template capsule. Pyridylphosphines, $P(Py)_3$, are successful template ligands as the imines of the pyridyl groups selectively coordinate to Zn^{II}-porphyrins or Zn^{II}-salphens, [Zn], resulting in the ligand–template capsule **G**, *i.e.* $P(Py)_3{\cdot}[Zn]_3$ (Fig. 5a). The zinc building blocks create a hemispherical capsule around the pyridylphosphines. The phosphine atoms of the pyridylphosphines can coordinate to a transition metal such as Rh or Pd which result in their encapsulation, *i.e.* [**G** ⊃ Rh or Pd] (this notation denotes that **G** encapsulates Rh or Pd). Addition of the zinc building blocks to the rhodium-bis-tris(*meta*-pyridyl)phosphine-complex, $Rh(P(m\text{-}Py)_3)_2(CO)(acac)$, creates sterical hindrance around the encapsulated metal and results in the decoordination of one of the two pyridylphosphine ligands to give $[P(m\text{-}Py)_3{\cdot}[Zn]_3 \supset Rh(CO)(acac)]$ *i.e.* [**G** ⊃ Rh(CO)(acac)] (Fig. 5b). The encapsulated rhodium catalysts were shown to have unusual reactivity and regioselectivity in the hydroformylation reaction (*vide infra*).

Reek and co-workers have also reported a ligand–template approach for metal encapsulation in which the ligand–template is an integrated part of the capsule.[32] This example involves a concave shaped bifunctional diphosphine ligand which can complex a transition metal and also contains functional groups for capsule formation. Self-assembly of the tetracationic diphosphine ligand with a tetraanionic calix[4]arene leads to the formation of a reversible hetero-capsule based on ionic interactions (**H**). Coordination of

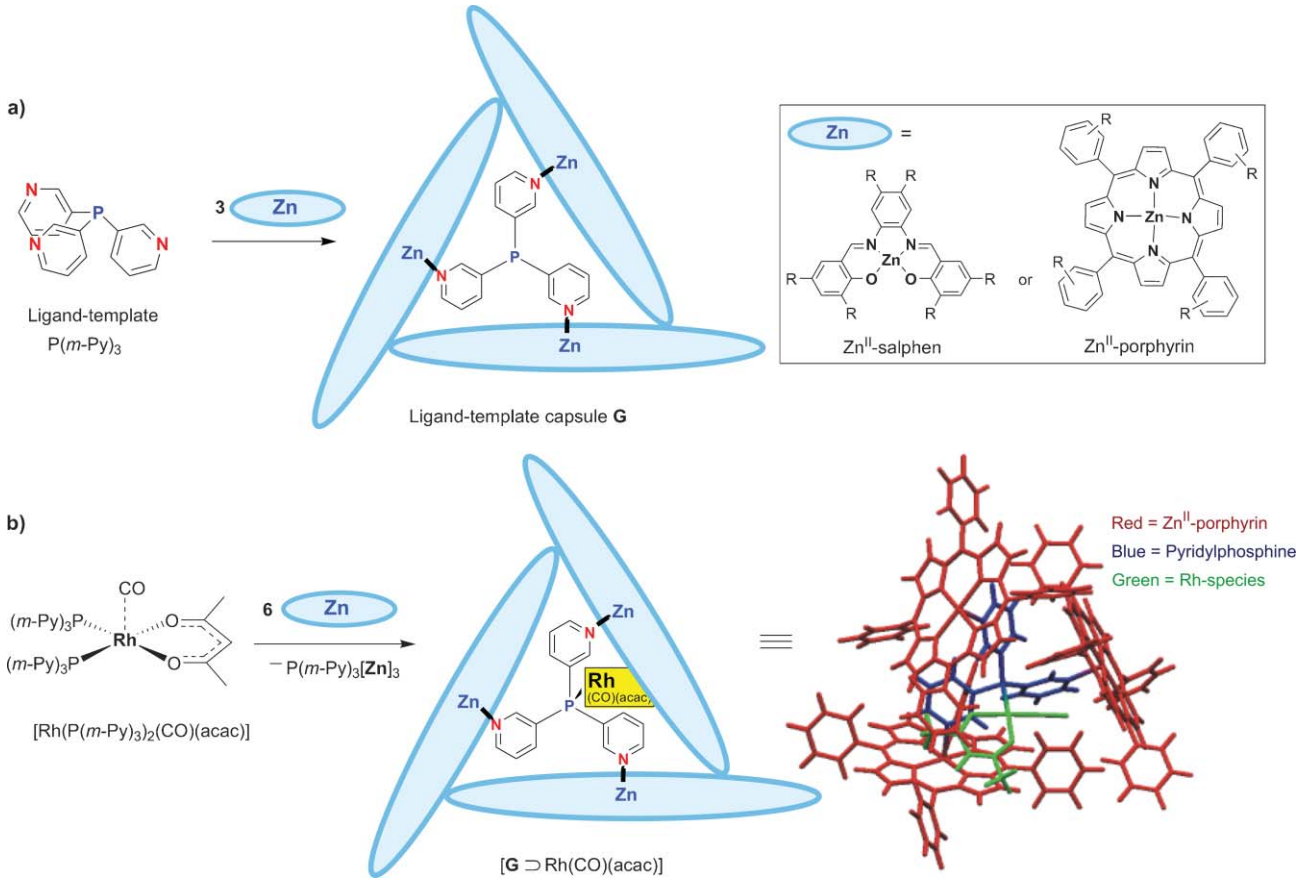

Fig. 5 a) Self-assembly of ligand–template capsule **G**. b) Encapsulation of a Rh-species within capsule **G**, *i.e.* [**G** ⊃ Rh(CO)(acac)] (modeling picture on the right). Reproduced in part with permission from Wiley InterScience from reference 27.

palladium to the template–ligand results in metal encapsulation [**H** ⊃ Pd–Ar] (Fig. 6).

4. Encapsulation effects in catalysis

The field of supramolecular catalysis has a long history and in many papers the analogy with enzymes is made. On the one hand this connection makes sense as enzymes have been a source of inspiration, on the other hand these comparisons are too general to be of scientific relevance. There are many different classes of enzymes that work with different mechanisms and principles, and also there are very active and rather slow enzymes and very selective and nonselective enzymes. In addition, the working principles of enzymes are still under debate. We therefore focus on a few principles that are found to be rather general for enzymes and can be expected to be also of relevance for reactions carried out in molecular capsules, *i.e.* nanoreactors. Enzymes recognize and bind substrates within their cavity near the catalytic centre. This results in substrate preorganization before the actual reaction takes place. The enzyme binds and stabilizes the transition state of the reaction better than the substrate by additional binding interactions (covalent or noncovalent interactions such as H-bonding and ionic interactions) and by having a complementary shape to the transition state. This decreases the energy barrier, which accounts for at least a part of the rate enhancement observed by enzymes. All other effects that are involved are either not general or hard to quantify.

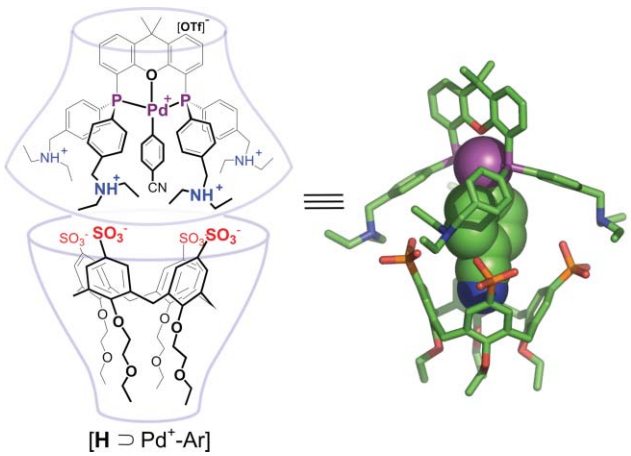

Fig. 6 Bisphosphine based heterocapsule **H** encapsulating a transition metal, [**H** ⊃ Pd–Ar], (modeling picture on the right). In the modeled structure, some substituents and hydrogen atoms have been omitted for clarity.

In the next paragraph we will have a closer look at the reaction rates of processes that take place inside and outside capsules. At this point it is important to realize that the selectivity of a reaction is a matter of relative reaction rates between competitive pathways. Also the isolation (or trapping) of otherwise unstable reaction intermediates by encapsulation

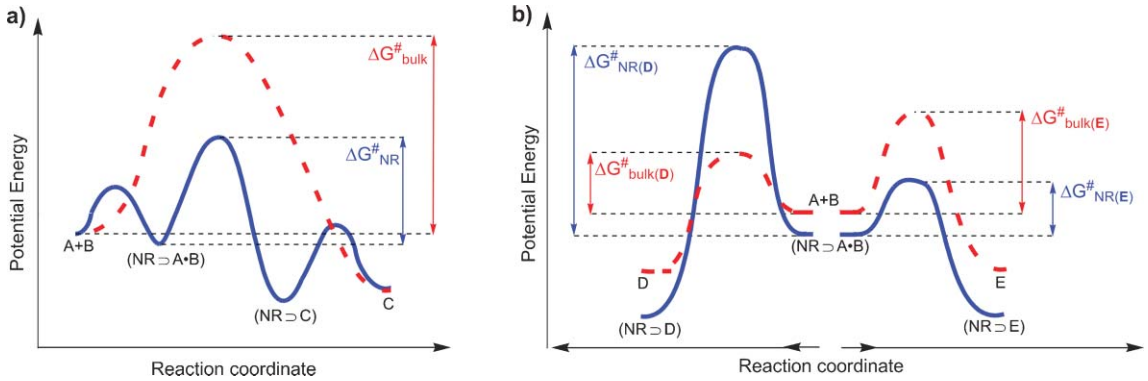

Fig. 7 a) Simplified reaction profiles of a reaction in the bulk solution (dashed red line) and of a reaction within a nanoreactor (blue line). b) Simplified reaction profiles of a reaction leading to product D which is destabilized by the nanoreactor (blue line) compared to the bulk solution (dashed red line), and of a reaction leading to product E which is stabilized by the nanoreactor (blue line) compared to the bulk solution (dashed red line).

and issues such as product inhibition can be explained in terms of reaction rates as this is a matter of changing the relative rate of a sequence of reaction steps. It is of great relevance to understand how the rate-equation of a reaction changes when the process takes place inside the capsule.

Encapsulation effects in terms of rate-equation

In order to understand encapsulation effects of chemical processes one should analyse the corresponding rate-equation rather than comparing nanoreactors to enzymes. For a simple bimolecular reaction where substrates A and B are giving product C (eqn 1) the general rate-equation can be used (eqn 2). If reactions take place inside a capsule one needs to take the substrate encapsulation and product release in-and-out of the nanoreactor (NR) into account, resulting in a more complex rate-equation as all three events have to be considered (eqn 3). In an ideal case where the reaction between A and B inside the nanoreactor (NR) is the rate determining step, the rate-equation simplifies analogously to Michaelis–Menten kinetics and depends solely on the rate-constant of this step, *i.e.* k_b, and on the capsule concentration with the encapsulated substrates (NR ⊃ A·B) (eqn 4).§ In terms of energy profiles these equations can be translated to the energy diagrams depicted in Fig. 7a.

$$A + B \xrightarrow{k_a} C \quad (1)$$

$$v = d[C]/dt = k_a[A][B] \quad (2)$$

$$NR + A + B \rightleftharpoons (NR \supset A{\cdot}B) \xrightarrow{k_b} (NR \supset C) \rightleftharpoons NR + C \quad (3)$$

$$v = d[C]/dt = k_b[(NR \supset A{\cdot}B)] \quad (4)$$

The rate-constant k is a function of the thermodynamic activation parameters, *i.e.* the Gibbs free energy of activation ($\Delta G^{\#}$) and hence to the activation enthalpy ($\Delta H^{\#}$) and the activation entropy ($\Delta S^{\#}$) *via* the Eyring and Arrhenius equations: $\Delta G^{\#} = \Delta H^{\#} - T\Delta S^{\#} = -RT(\ln k) + c$. ($T$ = temperature, R = gas constant, c = a constant).

Two extreme scenario's can be distinguished when reactions take place inside a capsule (in practice this might be a combination of the two):

1) The nanoreactor does not change the activation parameters (*i.e.* $\Delta G^{\#}_{NR} = \Delta G^{\#}_{bulk}$) and the only effect to be expected is the preorganization effect of bringing the substrates together. In essence, the reaction goes from a bimolecular to an intramolecular reaction pathway. Since the activation parameters in eqn (2) and (4) are the same, the rate constant remains the same, $k_a = k_b$, and the difference in the rate is due to the fact that: $[(NR \supset A{\cdot}B)] > [A][B]$. In this paper we will refer to this as *effective concentration*.[33] For a reaction that is carried out at a millimolar concentration, the increase in reaction rate will be a factor 1000 (using a millimolar capsule), whereas the increase in reaction rate at higher concentrations is much smaller. At extremely high substrate concentrations (above 1 molar) other issues will become important and the current simplification will no longer hold.

2) The nanoreactor does change the activation parameters (*i.e.* $\Delta G^{\#}_{NR} \neq \Delta G^{\#}_{bulk}$). Like enzymes, nanoreactors can *stabilize transition states* ($\Delta G^{\#}$) of the reactions taking place in the capsule, which lowers the reaction activation energy barrier (*i.e.* $\Delta G^{\#}_{NR} < \Delta G^{\#}_{bulk}$) as is depicted in Fig. 7a.[34] Besides the obvious enthalpic stabilization ($\Delta H^{\#}$) *via* noncovalent interactions between the transition state and the surrounding, entropy ($\Delta S^{\#}$) can also play a key role in this stabilization. The specific size, shape and chemical environment of the confined nanospace *preorganizes encapsulated substrates* towards the transition state by restricting their translational and rotational degrees of freedom and directing their orientation within the enclosed cavity. Generally, a precise fit between the cavity and the substrates results in a more effective preorganization, reducing the potential negative entropy of a reaction. The cavity can also activate substrates by forcing them to adopt the most reactive conformation of those populated in the bulk, *i.e.* statistic effect.[34]

§ An important difference between enzymes and nanoreactors is product release from the cavity. The Michaelis–Menten kinetics assumes that product release occurs rapidly (this assumption is also made in eqn 4). However, this assumption does not always count for nanoreactors because they can display product inhibition, *vide infra*.

New reactivities and selectivities

The specific size, shape and hydrophobic environment of the cavity as well as partial desolvation and isolation of the substrates from the bulk solvent can induce new activities and selectivities.[35] The new microenvironment within the nanoreactor can for example enforce the substrates to adopt conformations which are either not or less populated in the bulk or stabilize certain reactive intermediates. In bimolecular reactions the cavity can direct the relative spatial orientation of the two substrates, facilitating selective reactions by *e.g.* blocking bulk solution pathways that require an orientation which is not possible within the cavity.[36] Indeed, manipulation of reaction energetics and environment through encapsulation might provide access to reaction pathways which were otherwise inaccessible because of their high energy, *i.e.* the energy landscape within the nanoreactor might be different from the one outside. The former can be illustrated by considering a kinetically controlled reaction between A and B which can give two products: D and E. The specific interactions between the nanoreactor and the encapsulated substrates can alter the reaction activation energy barrier $\Delta G^{\#}$ of products D and E compared to the bulk. The transition state leading to product E can be stabilized upon encapsulation and thereby favouring its formation. In contrast, the transition state leading to product D can be destabilized upon encapsulation and thereby favouring the formation of the other product E (Fig. 7b). The former example describes a situation where the activity and selectivity of a reaction can be reversed upon replacing the bulk solvent with a nanoreactor.

Substrate size and shape selective reactions can also be explained in terms of effective concentration and transition state stabilization. 1) In a mixture of substrates a higher concentration can be achieved for those having a complementary size and shape to the nanoreactor portals and cavity (and thus can enter the nanoreactor) compared to the others that can not easily enter or do not fit within the cavity. In some cases, when the substrate encapsulation is a slow process (slow diffusion), substrate encapsulation can become the rate determining step. 2) One can also imagine that substrates of identical size and shape can both enter the cavity, but the transition state of one of the reaction pathways is stabilized to a greater extent than the other. Importantly, for all encapsulated reactions one should keep in mind that the substrate residence time within the nanoreactor and the kinetic rates of the encapsulated reaction should at least have a comparable magnitude.[37]

Product stabilization

Nanoreactors might give rise to *product inhibition* when the nanoreactor has a higher affinity for the product compared to the substrate(s). Inhibiting product release prevents a catalytic turnover or at least lowers the reaction rate. In the case of product inhibition, the encapsulated product, *i.e.* (NR $\supset$ C), is very low in energy and the barrier for product release from the nanoreactor cannot be overcome (Fig. 7a). This higher preference for the product can be enthalpic, the product has multiple attractive interactions with the host. Entropic disadvantages in bimolecular reactions arise from the need to replace a single product by two substrates, which can also contribute to product inhibition effects. In some cases, product inhibition can be skirt around, for example by having a subsequent reaction with the product to a second product that has lower affinity for the nanoreactor.[34] Product inhibition is occasionally observed in metallo-cages when the product is too large to leave the nanoreactor through its portals. This steric barrier can be overcome by using a more open shaped nanoreactor or by aiming for products that are too small to cause product inhibition.[36] The reverse has been shown for H-bonded capsules where a too large product enforced the capsule to (partly) open for guest exchange.[38] Interestingly, product inhibition can also be used for the stabilization of reactive intermediates, or labile products that are otherwise difficult to isolate and analyse.[39] The stabilization of reactive intermediates can provide new information on mechanism of the particular chemical reaction.

Nanoreactors with an active site

For nanoreactors with an *active site* such as transition metal species, similar effects as described above can be expected.[20,26,27] The rate equation (eqn 4) is of course different and it might include the catalyst concentration. However, the principles remain the same: capsules can bring reactant and catalyst together or the activation parameters can be modified. Transition metal-catalysed reactions consist of several steps, *i.e.* the catalytic cycle, with one of these steps being the rate determining step. The rate determining step of the catalytic cycle can change in the capsule compared with the bulk phase as a consequence of the change in activation parameters, resulting in new selectivities.[29] Also, the cavity can change the structure of the encapsulated active-site giving rise to inherently different properties.[30,31] Similar to above, the second coordination-sphere around the active site can induce substrate size-, shape-, and regio-selectivities. Active site encapsulation can also result in stabilization of the active site preventing catalyst decomposition. For transition metal catalysis this stabilization effect might be one of the driving forces towards future application.

5. Nanoreactors at work

Self-assembled capsules have been successfully applied as nanoreactors for various uni- and bimolecular reactions. The novel finite microenvironment within the nanocapsules and their reversible encapsulation properties have stimulated their application as nanoreactors. As is described below nanoreactors are used for thermal, photochemical and transition metal-catalysed reactions and induce novel properties such as substrate size and shape selectivities, and product chemo-, regio- and stereoselectivities. In some examples the nanoreactors served as catalysts, whereas in others the encapsulated reaction appeared to be stoichiometric. In this section literature examples are given of chemical conversions within these nanoreactors. In the first part the stoichiometric reactions are discussed, next we will elaborate on catalytic events and in the final section catalysis with encapsulated active-sites will be discussed.

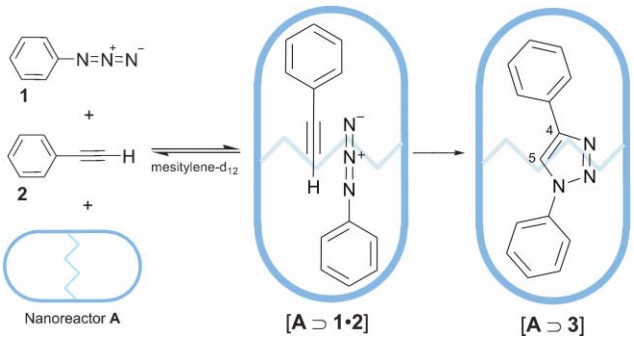

Scheme 1 1,3-Dipolar cycloaddition between phenylazide **1** and phenylacetylene **2** within nanoreactor **A**.

5.1 Stoichiometric reactions within nanoreactors

1,3-Dipolar cycloaddition. Rebek and co-workers have applied the cylindrical capsule **A** as a nanoreactor for the 1,3-dipolar cycloaddition between phenylazide **1** and phenylacetylene **2** (Scheme 1).[40] Nanoreactor **A** simultaneously encapsulates reagents **1** and **2** to give [**A**⊃ **1**·**2**] (this notation denotes that **A** encapsulates **1** and **2**) next to the homo combinations [**A** ⊃ $\mathbf{1_2}$] and [**A** ⊃ $\mathbf{2_2}$] which are present slightly less than the statistical distribution would predict. It was shown that the cylindrical cavity of **A** constrains the guests orientation edge-to-edge so that their substituents make contact. The cycloaddition within nanoreactor **A** results exclusively in 1,4-triazole **3** after several days at millimolar concentrations. In contrast, the reaction in the absence of **A** produces a 1 : 1 mixture of regioisomeric products of 1,4- and 1,5-triazoles and has a half-life of several years. The observed rate enhancement is explained by an effective concentration of 3.7 M within **A**. The high regioselectivity results from preorganized substrates orientation within **A**, imposed by the nanoreactor boundaries. Nanoreactor **A** has also shown to be substrate size selective; the encapsulated cycloaddition between the larger azides 1-naphthyl azide or 4-biphenyl azide and phenylacetylene was not accelerated. The system suffers from product inhibition and therefore stoichiometric amounts of **A** have to be used. The product could be liberated upon addition of DMF resulting in denaturation of the capsule.

Diels–Alder reaction. The octahedral coordination cage **D** described by Fujita and co-workers has been applied as a nanoreactor for the bimolecular Diels–Alder reaction in water.[36] Nanoreactor **D** can selectively pairwise recognize two different substrates. Suspending 9-(hydroxymethyl)-anthracene **4** and *N*-cyclohexylmaleimide **5a** in an aqueous solution of near-stoichiometric quantities of **D** has resulted in the selective formation of [**D** ⊃ **4**·**5a**] (Scheme 2a). Upon warming the reaction mixture, the Diels–Alder product **6a** is formed in >98% and could be isolated by extraction with chloroform. The nanoreactor has induced a unusual regioselectivity by promoting a reaction at the terminal anthracene ring to give the *syn*-1,4-Diels–Alder adduct **6a**, while free solution reaction yields the product bridging at the central anthracene ring, the 1,9-Diels–Alder adduct, in 44%. The unusual stereo- and regioselectivity in the encapsulated Diels–Alder reaction is explained by the fixed orientation of the two substrates within **D**, preventing interaction at the 9,10 position of the anthracene **4**. This is an example where preorganization within the nanoreactor prevents the most energetically favoured product. However, product inhibition by strong complexation of **6a** within **D** prevents a catalytic turnover.

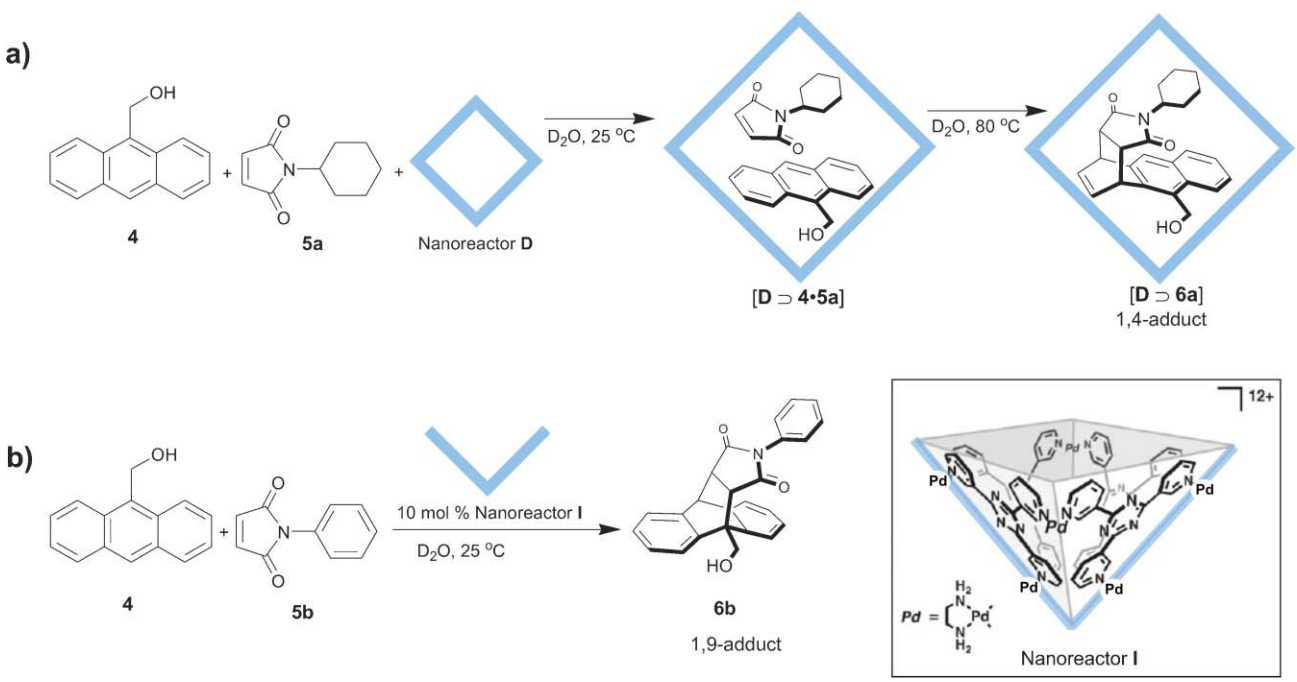

Scheme 2 a) Diels–Alder reaction between the anthracene **4** and *N*-cyclohexylmaleimide **5a** within nanoreactor **D**. b) Catalytic Diels–Alder reaction between the anthracene **4** and *N*-phenylmaleimide **5b** within nanoreactor **I**. On the right: square-pyramidal bowl **I** (M_6L_4). Reproduced in part with permission from Science from reference 36.

Interestingly, the Diels–Alder reaction of the anthracene **4** and *N*-phenylmaleimide **5b** could be catalysed with a turnover using 10 mol% of a square-pyramidal bowl **I**. In this reaction the conventional regiochemistry of the 1,9-Diels–Alder adduct **6b** (Scheme 2b) was obtained. Bowl **I** does not suffer from product inhibition because its open structure allows facile guest exchange (no kinetic traps), and the affinity for the substrate and product is based on aromatic stacking, which is more pronounced for the substrate than product **6b**. It is unknown if the rate acceleration is caused by effective concentration and/or transition state stabilization.

Remarkably, nanoreactor **D** can also efficiently promote the Diels–Alder reaction of highly stable and relative inert aromatic molecules such as triphenylene and perylene with **5a** to give the corresponding endo Diels–Alder adduct with the *syn* stereochemistry in high yields.[42] The steric demand of the *N*-cyclohexyl group on **5a** is important as it directs the orientation of the substrate within the cavity of **D**.

Olefin photodimerization. The octahedral coordination cage **D** has been used by Fujita and co-workers as a nanoreactor for the bimolecular [2 + 2] photodimerization of olefins.[43] Suspending bulky olefins such as acenaphthylenes **7a** or **7b** in an aqueous solution of **D** resulted in complexes [**D** ⊃ (**7a**)$_2$] and [**D** ⊃ (**7b**)$_2$], respectively (Scheme 3a). Isolation and irradiation of these complexes yielded the encapsulated *syn*-dimers [**D** ⊃ **8a**] and [**D** ⊃ **8b**] in >98%. The products were isolated by extraction with chloroform. Compared to the solution phase photodimerization of **7a** in benzene, the nanoreactor has accelerated the reaction and improved the stereoselectivity for the *syn*-dimer **8a** from 53% to 100%. In addition, the nanoreactor protects the encapsulated product **8a** against photodissociation. Photodimerization of the nonsymmetrically substituted 1-methylacenaphthylene **7b** can result in four different isomers. Under standard conditions, however, no dimerization occurs due to the steric hindrance of the methyl group, but photodimerization of **7b** within nanoreactor **D** does occur with a high stereo- and regioselectivity as is demonstrated by the exclusive formation of the head-to-tail *syn*-dimer **8b**.

The cross-photodimerization reaction represents a great challenge because it requires **D** to selectively pairwise recognize two different olefins prior to irradiation when the cross-coupling reaction under standard conditions has no preference above the homo-coupling. The cross-photodimerization of acenaphthylene with substituted naphthoquinones within **D** resulted in exclusive formation of the cross *syn*-dimer only for 5-ethoxynaphthoquinone, while the less steric olefins having a 5-methoxy or no substituent also gave homodimers besides heterodimers (Scheme 3b).[44] In addition, even relatively inert polycyclic aromatic compounds such as pyrene, phenanthrene and fluoranthene were selectively [2 + 2] cross-photodimerized with *N*-cyclohexylmaleimide within **D**, resulting in high stereo- and regioselectivity.[42] Again, the steric demand of the *N*-cyclohexyl group of the maleimide is essential, as less sterically demanding groups were not reactive in the photodimerization with pyrene.

Substrates desolvation and the hydrophobic environment within the cavity creates a *new inner phase* for new applications. Indeed, the water-soluble nanoreactor **D** with a hydrophobic cavity has been used as phase-transfer catalysts for Wacker oxidation of styrene in an aqueous phase.[45] Another interesting feature of nanoreactors is their molecular frame that can play an active role in the encapsulated reaction. The triazine ligands of Fujita octahedral cage **D** for example can be photochemical excited and subsequently electron

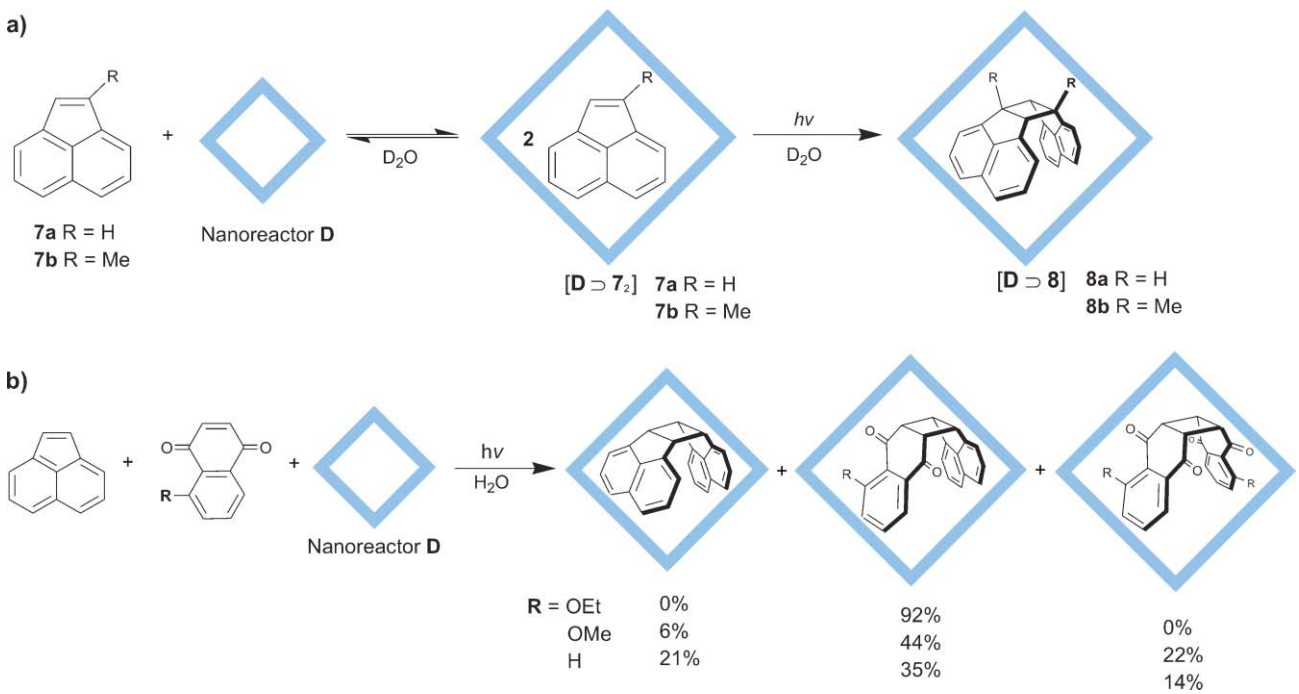

Scheme 3 a) Photodimerization of acenaphthylenes **7a** or **7b** within nanoreactor **D**. b) Cross-photodimerization between acenaphthylene and substituted 1,4-naphthoquinone within nanoreactor **D** (product distribution).

transfer from the encapsulated alkane to the cage induces substrate oxidation.[46] As mentioned previously, nanoreactors can also stabilize *in-situ* generated reactive intermediates and labile products like in the oligomerization of trialkoxysilanes within **D**, which could not be isolated without being stabilized within the nanoreactor.[39]

Photo-oxidation. The cavitand-based capsule **E** has been applied by Ramamurthy and co-workers as a nanoreactor for the oxidation of methyl cycloalkenes by singlet oxygen to give allylic hydroperoxides.[47,48] Addition of one equivalent of 1-methylcyclohexene **9** to one equivalent of the deep-cavity cavitand in a basic aqueous solution (which is necessary for capsule formation) resulted in the formation of nanoreactor **E** encapsulating two substrate molecules, *i.e.* [**E** ⊃ $\mathbf{9}_2$] (Scheme 4a). In the photo-oxidation reaction a singlet oxygen ($^1O_2$) is added to the alkene bond and simultaneously one of the allylic hydrogens is abstracted, which can result in three different allylic hydroperoxides **10a**, **10b** and **10c** (Scheme 4a). Two different photosensitizers were used to generate singlet oxygen, namely the water soluble Rose Bengal (RB) or the water insoluble dimethylbenzil (DMB). In the later case, DMB was itself encapsulated within nanoreactor **E** [**E** ⊃ DMB], *vide infra*. Irradiation of [**E** ⊃ $\mathbf{9}_2$] in the presence of photosensitizer RB or [**E** ⊃ DMB] yielded the allylic hydroperoxides **10a** and **10c** in 60–70% with 90–95% selectivity towards the regioisomer **10c**. The products were isolated by extraction with chloroform. As can be seen in Scheme 4a, in the absence of nanoreactor **E** (in acetonitrile with photosensitizer RB) three hydroperoxides are formed, **10a** (44%), **10b** (20%) and **10c** (36%). The unusual high preference of the nanoreactor towards product **10c** points out the high regioselectivity induced by the nanoreactor in this oxidation reaction. The authors have concluded from NMR studies that the methyl groups of the encapsulated substrates are anchored at the narrowest parts of the nanoreactor (Scheme 4a). Hence, the encapsulated substrate is oriented as such that singlet oxygen is prevented from approaching the methyl group. It is important to note that it is very difficult to control selectivity in reactions with singlet oxygen. In addition, the NMR studies also support the observations that the allylic hydrogen H_3 of **9** is the most accessible of the three allylic hydrogen sets (H_3, H_6 and H_7). Interestingly, nanoreactor **E** also stabilizes the product because the encapsulated hydroperoxides [**E** ⊃ $\mathbf{10}_2$] remained stable for weeks.

A very interesting aspect of this study is the use of the photosensitizer dimethylbenzil (DMB). This photosensitizer does not dissolve in water, unless it is encapsulated within nanoreactor **E**, [**E** ⊃ DMB] (Scheme 4b). It is important to notice that when [**E** ⊃ DMB] and [**E** ⊃ $\mathbf{9}_2$] were mixed no guest exchange was observed and the capsules remained independent. The oxidation reaction of **9** involving [**E** ⊃ DMB] starts with the generation of excited DMB, *i.e.* [**E** ⊃ *DMB]. Next, the former nanoreactor opens and allows contact between oxygen and *DMB, resulting in the formation of singlet oxygen ($^1O_2$). In a subsequent step, the singlet oxygen exits [**E** ⊃ DMB] and enters [**E** ⊃ $\mathbf{9}_2$] which results in regioselective oxidation of **9**. This system has properties related to those important for biological signaling.[48]

5.2 Catalysis by nanoreactors

Diels–Alder reaction. Rebek and co-workers have used "softball" **B** as a nanoreactor for bimolecular Diels–Alder

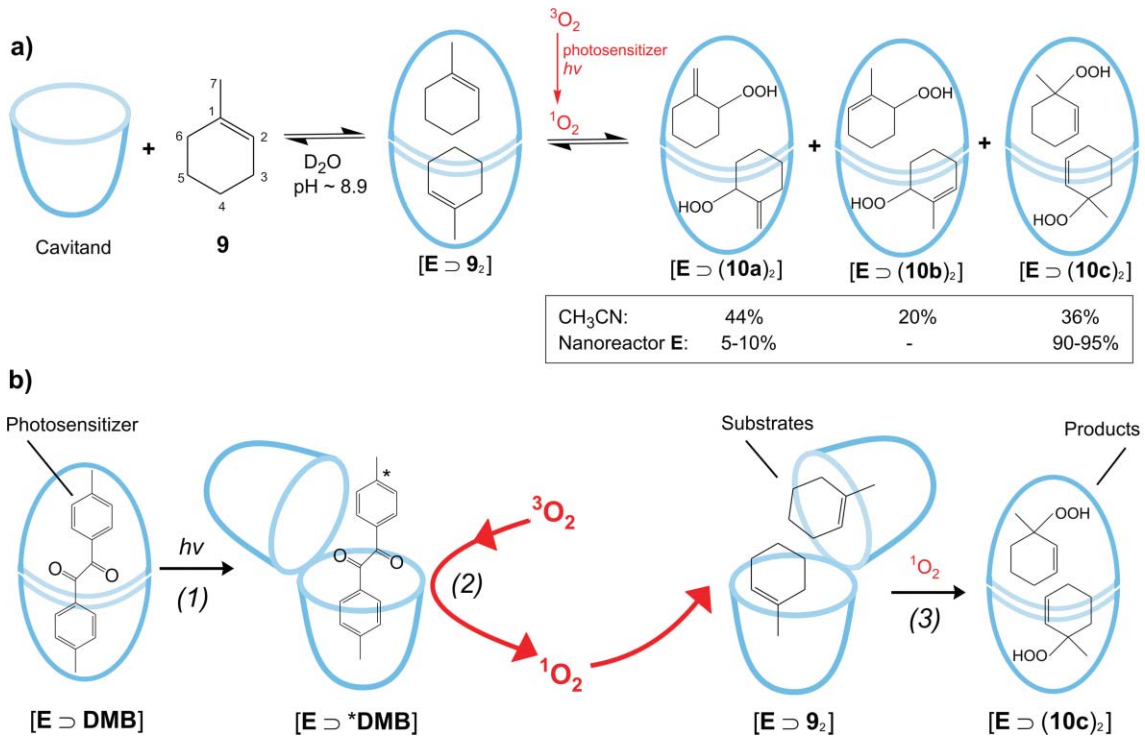

Scheme 4 a) Photo-oxidation of 1-methylcyclohexene **9** within nanoreactor **E**. b) *1.* Excitation of an encapsulated photosensitizer [**E** ⊃ DMB]. *2.* Excitation of triplet oxygen by an encapsulated photosensitizer [**E** ⊃ *DMB]. *3.* Photo-oxidation of encapsulated **9** [**E** ⊃ $\mathbf{9}_2$] by singlet oxygen.

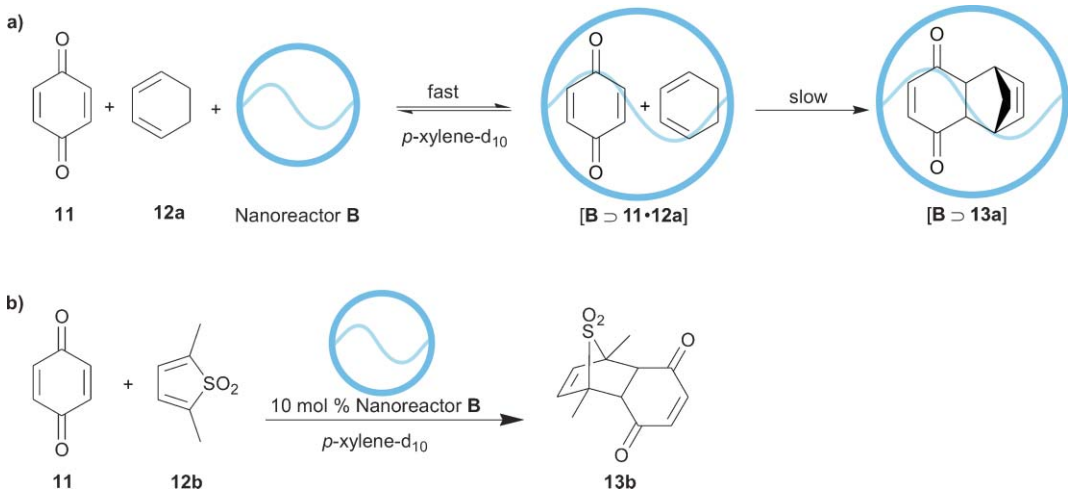

Scheme 5 a) Diels–Alder reaction between *p*-benzoquinone **11** and cyclohexadiene **12a** within nanoreactor **B**. b) Catalytic Diels–Alder reaction between *p*-benzoquinone **11** and the thiophene dioxide derivative **12b** within nanoreactor **B**.

reactions.[38] The Diels–Alder reaction between *p*-benzoquinone **11** and cyclohexadiene **12a** within nanoreactor **B**, present in stoichiometric amounts, has been accelerated 170-fold compared to the bulk and resulted in the encapsulated adduct [**B** ⊃ **13a**] (Scheme 5a). Even though nanoreactor **B** enhances the rate of the encapsulated reaction, no true catalytic behaviour was observed because of product inhibition by **13a**. Product inhibition is partly suppressed if thiophene dioxide derivative **12b** is used as the diene (Scheme 5b). This is because the Diels–Alder product of the thiophene dioxide derivative **13b** has a lower affinity for nanoreactor **B** than two equivalents of the *p*-benzoquinone **11**, *i.e.* [**B** ⊃ (**11**)$_2$] have. After encapsulating two quinones **11** within **B** one of them is occasionally replaced by a thiophene dioxide **12b**, which leads to the encapsulated Diels–Alder product **13b**. After each turnover the encapsulated product is released and replaced by two quinone reactants and true catalysis can take place. When using catalytic amounts of **B** (10 mol%) a tenfold rate enhancement (at 10 mM substrate concentration) compared to the background reaction was observed, which is still lower than can be expected on the basis of the effective concentration.

Hydrolysis. The tetrahedral coordination cage **C** has been used by Raymond, Bergman and co-workers as a catalyst for the acidic hydrolysis of orthoformates in basic solutions.[49] This is an example where the new inner phase facilitates reactions which are not possible in the exterior environment. Nanoreactor **C** has a much higher affinity for monocationic guests over neutral guests. Addition of neutral and even weakly basic compounds such as amines, phosphines and orthoformates, $HC(OR)_3$, to aqueous solutions of **C** resulted in encapsulation of their protonated form. The protonation is thermodynamically driven by stabilization of the protonated species. Hydrolysis of orthoformates involves a protonated intermediate. Indeed catalytic amounts of **C** (1 mol%) in basic solution (pH 11) gave rapid hydrolysis of orthoformates to the corresponding formate esters, HC(O)(OR), which is subsequently hydrolysed by OH^- to formate, HCO_2^- (Scheme 6a). Product inhibition is not taking place and the empty nanoreactor **C** can re-enter the catalytic cycle like a true catalyst. Rate accelerations of up to 890-fold were observed for triisopropyl orthoformate. As expected, nanoreactor **C** exhibits substrate size selectivity and only orthoformates smaller than tripentyl orthoformate are readily hydrolysed.

A mechanistic study of the catalytic reaction has revealed a catalytic cycle in which the neutral orthoformate is first encapsulated within nanoreactor **C** (Scheme 6b). Protonation of the encapsulated substrate, presumably by deprotonation of water, results in the stabilized monoprotonated orthoformate. Subsequently, two successive hydrolysis steps within **C** liberate two equivalents of the corresponding alcohol. Finally, the protonated formate ester is ejected from **C** and is further hydrolysed by OH^- in solution. The shift in the effective basicity of the encapsulated guests compared to the free analogue is four orders of magnitude, typically also found for enzymes that modify basic properties of the encapsulated substrates. This example is clearly based on stabilization of the transition state by interactions between the capsule and the encapsulated transition state. The mechanism of the encapsulated reaction involves an initial pre-equilibrium step followed by a first-order rate-limiting step. This Michaelis–Menten kinetics is parallel to enzymatic pathways. An inhibition study with NPr_4^+, a strongly and reversible guest for **C**, has revealed that the encapsulated hydrolysis reaction exhibits competitive inhibition.

The unimolecular Aza-Cope rearrangement of allyl enammonium cations within nanoreactor **C** was also investigated by Raymond, Bergman and co-workers.[20,34] The reaction was catalysed by 13 mol% of **C** and a rate acceleration of up to 850-fold was observed. The nanoreactor induced substrate size and shape selectivities. The nanoreactor acted as a true catalyst, since release and hydrolysis of the iminium product has circumvented product inhibition. Since this is an intramolecular reaction, this is a clear-cut example in which the capsule preorganizes the substrate to reduce the entropic contributions to the activation energy.

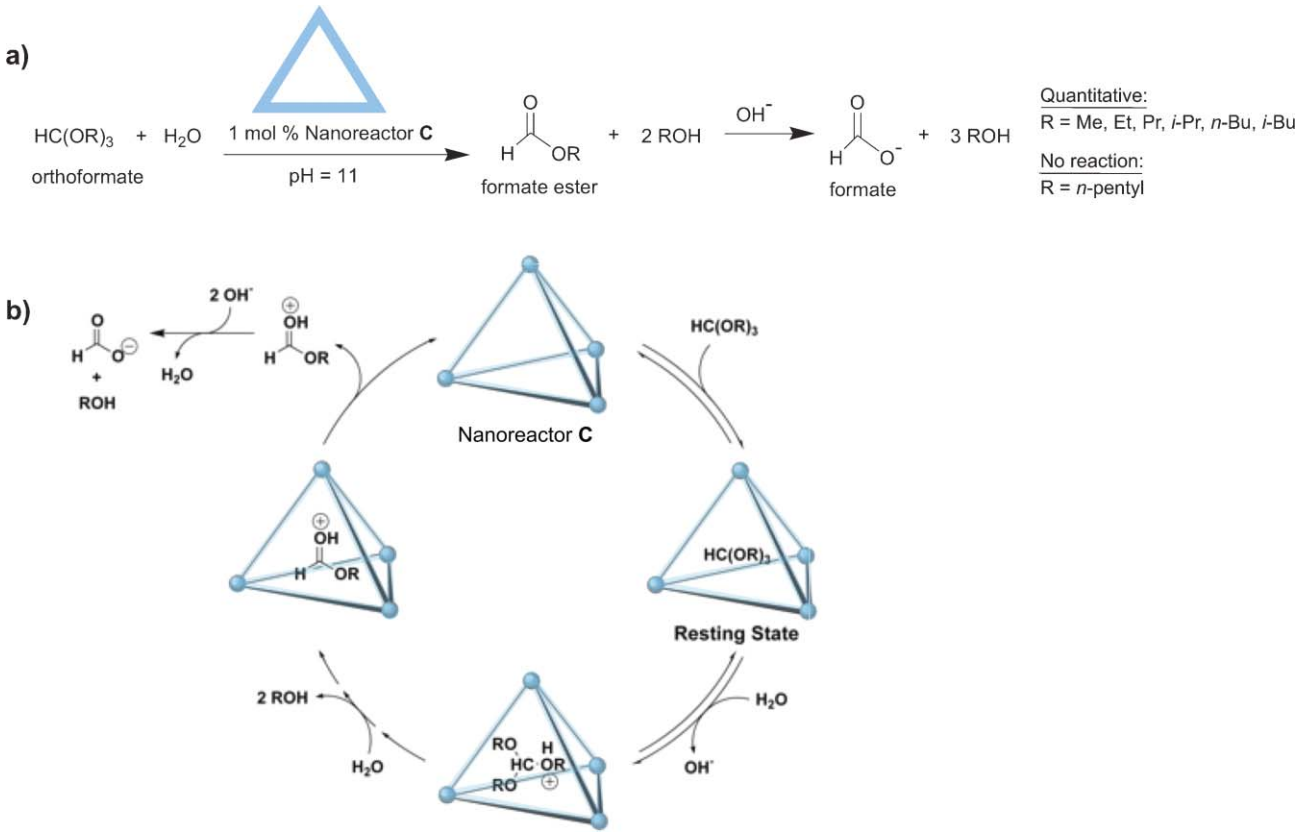

Scheme 6 a) Catalytic hydrolysis of orthoformates within nanoreactor **C**. b) Mechanism for catalytic orthoformate hydrolysis within **C**. Reproduced in part with permission from Science from reference 49.

5.3 Nanoreactors with encapsulated active sites

Allylic alcohol isomerization. Raymond, Bergman and co-workers have used a cationic rhodium complex encapsulated within the tetrahedral coordination cage **C** as an isomerization catalyst for allylic alcohols (Table 1).[25] The size selection by nanoreactor **C** only allowed the encapsulation of the catalyst precursor $[(PMe_3)_2Rh(COD)]^+$ and not the PEt_3-equivalent. The encapsulated precursor was hydrogenated to give the encapsulated active catalyst $[\mathbf{C} \supset (PMe_3)_2Rh(OD_2)_2^+]$, *i.e.* **[C ⊃ 14]**, which remained encapsulated for 12 h. **[C ⊃ 14]** is not the thermodynamic product as longer reaction times results in release of **14** from the capsule. Therefore, the application of **[C ⊃ 14]** is restricted to fast reactions such as allylic alcohol isomerization where substrate entrance and product release are rapid and occur prior to active site release. In contrast to the non-encapsulated catalyst **14**, the encapsulated catalyst **[C ⊃ 14]** only isomerized small allyl alcohols (Table 1, entry's 1b–3b). Encapsulation within nanoreactor **C** impose substrate size and shape selectivities to the active site. The origin of these selectivities lies in the apertures of the cage, which inhibit inclusion of larger branched substrates. It was known that the terminal substituted crotyl alcohol inhibits the catalyst (Table 1, entry 4a). Indeed, addition of both allyl alcohol and crotyl alcohol to the free catalyst **14** did not result in isomerization of either substrates. However, addition of both allyl alcohol and crotyl alcohol to **[C ⊃ 14]** resulted in the selective isomerization of the allyl alcohol. Hence, nanoreactor **C** protects the encapsulated catalyst **14** against decomposition by preventing the catalyst poison to interact with the catalyst.

Raymond, Bergman and co-workers have also studied the thermal C–H bond activation of aldehydes and ethers by an Ir(III)-complex encapsulated within nanoreactor **C**. This encapsulated iridium complex **[C ⊃ Ir-complex]** induced a

Table 1 Catalytic isomerization of allylic alcohols by **14**, $[(PMe_3)_2Rh(OD_2)_2^+]$, in bulk-solution or within nanoreactor **C**: **[C ⊃ 14]**

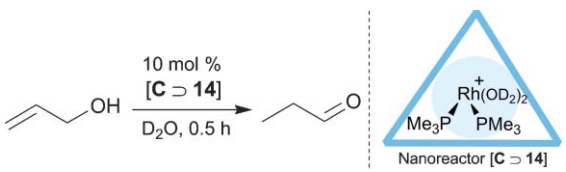

Entry	Substrate	Catalyst	Yield
1a		**14**	95%
1b		**[C ⊃ 14]**	95%
2a	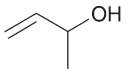	**14**	95%
2b		**[C ⊃ 14]**	n.r.
3a	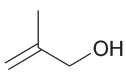	**14**	95%
3b		**[C ⊃ 14]**	n.r.
4a	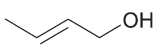	**14**	n.r.
4b		**[C ⊃ 14]**	n.r.

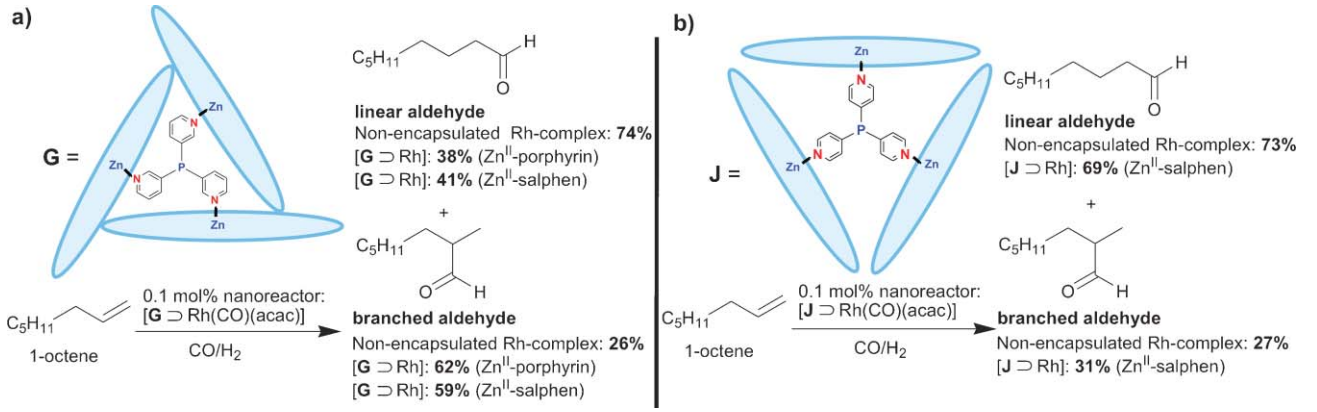

Scheme 7 Hydroformylation of 1-octene a) within nanoreactor [**G** ⊃ Rh] and b) within nanoreactor [**J** ⊃ Rh]. Product distribution of the aldehyde products.

highly specific substrate size and shape selectivities. However, product inhibition has prevented a catalytic turnover.[20,24]

Hydroformylation. Transition metal catalysts encapsulated within the ligand–template nanoreactor **G**, $P(Py)_3{\cdot}[Zn]_3$, have been applied by Reek and co-workers to catalyse industrially relevant processes such as hydroformylation and Heck reaction (for **G** see Scheme 7a or Fig. 5a).[29–31] Nanoreactor [**G** ⊃ Rh(CO)(acac)] encapsulates a Rh-species that contains only one tris(*meta*-pyridyl)phosphine ligand, P(*m*-Py)$_3$, surrounded by three Zn-porphyrins or Zn-salphens, as explained in Section 3. Under syngas pressure (H_2/CO) rhodium species like $Rh(CO)(acac)P(Py)_3$ transform in $HRh(CO)_3P(Py)_3$ species, which is the active species for the hydroformylation reaction. In this reaction terminal alkenes are converted into linear or branched aldehydes, and the ratio of these products strongly depends on the catalyst applied. Hydroformylation of 1-octene by encapsulated rhodium, [**G** ⊃ $HRh(CO)_3$], results in a 10-fold rate enhancement compared to the non-encapsulated rhodium catalyst (Scheme 7a).[30,31] In addition, the selectivity for the product has reversed; nanoreactor [**G** ⊃ $HRh(CO)_3$] containing Zn^{II}-porphyrins provides 63% of the branched aldehyde compared to 26% observed for the non-encapsulated species. The unusual selectivity and increased rate can only partly be explained by modification of the catalytically active species upon encapsulation. Indeed, upon encapsulation the rhodium complex goes from bisphosphine to monophosphine, which generally produce more branched aldehydes along with higher rates compared to the bisphosphine species. In addition, a part of the effect was ascribed to completely encapsulating the catalyst, as open cage analogues containing only two porphyrins instead of three, also have only one phosphine coordinated to the rhodium, but they are less active and produce much less branched aldehyde.

An advantage of the ligand-template approach for capsule assembly is the possibility to modify the capsule's shape by only minor changes of the template–ligand. This is demonstrated by meta- and para-trispyridylphosphines which were used as template–ligands. Addition of Zn^{II}-salphens to the *meta*- and *para*-trispyridylphosphines results in nanoreactors **G** and **J** respectively (Scheme 7).[30] Hydroformylation of 1-octene by the tris(*meta*-pyridyl)phosphine based nanoreactor [**G** ⊃ Rh] gave a preference for the branched aldehyde (Scheme 7a), whereas the tris(*para*-pyridyl)phosphine based nanoreactor [**J** ⊃ Rh] gave predominantly the linear aldehyde like the non-encapsulated bisphosphine–Rh–complex (Scheme 7b). These selectivities imply that nanoreactor [**G** ⊃ Rh] corresponds to a monophosphine–Rh–complex whereas nanoreactor [**J** ⊃ Rh] corresponds to bisphosphine–Rh–complex. The more open structure of nanoreactor **J** allows the formation of bisphosphine complexes while nanoreactor **G** forms a more enclosed cavity preventing bisphosphine species to form.

More recently, nanoreactor [**G** ⊃ Rh] has operated as a high-precision catalyst for the regioselective hydroformylation of internal alkenes.[29] The non-encapsulated $HRh(P(m\text{-}Py)_3)_2(CO)_2$ complex converts 2-octene to a near statistical mixture of the two expected internal aldehydes 2-methyloctanal and 2-ethylheptanal. However, nanoreactor [**G** ⊃ Rh], encapsulating the Rh-catalyst, has a strong preference to form 2-ethylheptanal (in 88%) (Scheme 8). This outstanding selectivity is unprecedented in the hydroformylation of internal alkenes. A similar selectivity was found in the hydroformylation of 3-octene. Experiments using various partial H_2 and CO pressures resulted in the proposition that the hydride migration is the selectivity-determining step. This step requires a rotation of the coordinated alkene which is hampered by the

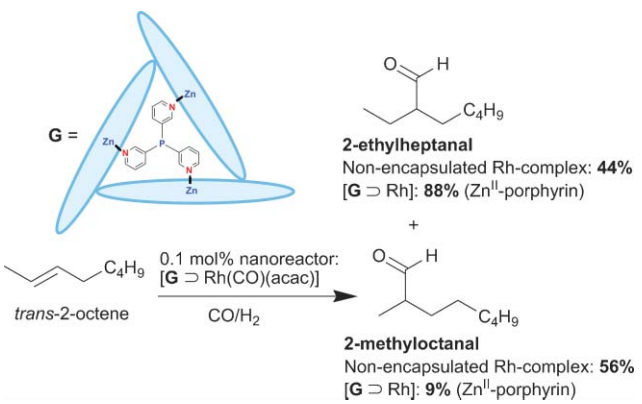

Scheme 8 Hydroformylation of *trans*-2-octene by nanoreactor [**G** ⊃ Rh]. Product distribution of the aldehyde products.

steric restrictions imposed by the innerside of the capsule. Apparently, rotation of the intermediate olefin complex leading to the 2-ethylheptanal product is more facile explaining the observed regioselectivity. Therefore it can be concluded that the nanoreactor determines the regiochemical outcome of the reaction by imposing its steric restrictions during a specific step in the catalytic sequence. It is interesting to note that there are no other reactions that can distinguish between the two carbon atoms of 3-octene, demonstrating that reactions carried out in nanoreactors can results in unprecedented selective reactions.

6. Conclusions and outlook

A wide array of self-assembled molecular capsules based on various building blocks and noncovalent interactions has been developed in the last decade. The nanospace within these supramolecular capsules is generally in the range of 300–500 $Å^3$, which is sufficient for the selective encapsulation of one large or a number of smaller molecules. The structure of the different capsules varies significantly, and as a result guest shielding and guest exchange rates strongly depend on the capsule applied. A diversity of chemical processes have been carried out within molecular capsules and the effects observed so far are, although academic, very interesting. Reactions can be *accelerated* and the *selectivity* of a chemical process can be changed completely. These observations can be explained by stabilization of the reaction transition state by the capsule (based on enthalpic and entropic contributions) or by concentration effects in the case of bimolecular reactions, such as Diels–Alder reactions. More important are the unique reaction *selectivities* induced by the novel finite microenvironment within the capsule. The size and shape of the nanoreactor's cavity and that of the nanoreactor's gates can control the substrate selectivity by controlling the access to the cavity. In a same manner it can protect an *active-site* located in the cavity that otherwise would be poisoned by chemicals present in solution. The *regio* and *chemo* selectivities can also be changed by the capsule by changing the ratio of reaction rates of competing pathways. This was for example observed for encapsulated rhodium complexes that were used as hydroformylation catalysts. In addition to these effects, reaction *intermediates* have been observed in nanoreactors that otherwise have too short lifetimes for identification. In these occasions the reaction rate of the subsequent step after the formation of the intermediate is slowed down by the nanocapsule. *Product inhibition*, which is a frequently encountered problem in bimolecular coupling reactions carried out within enclosed cavities, is fundamentally related to the former. The coupling product might have a higher affinity for the capsule than the substrates, and consequently product release from the nanoreactor becomes the slowest step in the reaction. Product inhibition can prohibit the utility of nanoreactors as true catalysts.

In addition to the nanoreactors discussed in this review, which are formed by assembly of at least two building blocks, capsules based on covalent bonds have also been applied as nanoreactors. These covalent nanoreactors are beyond the scope of the current review, but similar effects in catalysis are observed. However, self-assembled capsules also have guest exchange mechanisms *via* partial disassembly of the capsule, whereas exchange for the covalent analogues is restricted to portal slippage. It is this unique property that enables the combination of complete encapsulation with sufficiently fast in–out exchange, which might prove to be the advantage in the catalysis application. Future research should demonstrate these potential advantages.

Although the research field is still in its infancy, several examples of reactions carried out within self-assembled nanoreactors appeared and demonstrate the power of the concept. Detailed studies are required to fully understand the mechanisms behind the effects observed when carrying out reactions in nanoreactors. The results obtained so far sketch a bright prospective as reactions have been observed that are unique to those carried out in capsules. In this review we have focused on reactions that take place *inside* the capsules. However, molecular capsules have also been used to control reactions that take place *outside* the capsule for example by controlling the release of reagents, making the nanoreactor applications virtually unlimited.[41]

Acknowledgements

We thank the Netherlands Organization of Scientific Research (NWO, VICI grant), National Research School Combination Catalysis (NRSCC), and the University of Amsterdam for financial support, and all co-workers, whose names appear in the references, for their contributions.

References

1 P. W. N. M. van Leeuwen, *Homogeneous Catalysis: Understanding the Art*, Kluwer Academic Publishers, Dordrecht, The Netherlands, 2004; *Handbook of Homogeneous Hydrogenation, 3 Volumes*, ed. J. G. de Vries and C. J. Elsevier, WILEY-VCH, Weinheim, Germany, 2006.
2 *Enantioselective Organocatalysis: Reactions and Experimental Procedures*, ed. P. L. Dalko, WILEY-VCH, Weinheim, Germany, 2007; A. Berkessel and H. Groger, *Asymmetric Organocatalysis: From Biomimetic Concepts to Applications in Asymmetric Synthesis*, WILEY-VCH, Weinheim, Germany, 2005.
3 *Enzyme Catalysis in Organic Synthesis: A Comprehensive Handbook, 2nd*, ed. K. Drauz and H. Waldmann, WILEY-VCH, Weinheim, Germany, 2002.
4 L. Pauling, *Nature*, 1948, **161**, 707.
5 J. K. M. Sanders, *Chem.–Eur. J.*, 1998, **4**, 1378; A. J. Kirby, *Angew. Chem., Int. Ed. Engl.*, 1996, **35**, 707; W. B. Motherwell, M. J. Bingham and Y. Six, *Tetrahedron*, 2001, **57**, 4663.
6 J. Gao, S. Ma, D. T. Major, K. Nam, J. Pu and D. G. Truhlar, *Chem. Rev.*, 2006, **106**, 3188; M. J. S. Dewar and D. M. Storch, *Proc. Natl. Acad. Sci. U. S. A.*, 1985, **82**, 2225; X. Zhang and K. N. Houk, *Acc. Chem. Res.*, 2005, **38**, 379.
7 D. M. Vriezema, M. C. Aragones, J. A. A. W. Elemans, J. J. L. M. Cornelissen, A. E. Rowan and R. J. M. Nolte, *Chem. Rev.*, 2005, **105**, 1445.
8 A. Lützen, *Angew. Chem., Int. Ed.*, 2005, **44**, 1000.
9 J. M. Lehn, *Science*, 1985, **227**, 849.
10 J. M. Lehn, *Supramolecular Chemistry: Concepts and Perspectives*, WILEY-VCH, Weinheim, Germany, 1995.
11 D. J. Cram, *Science*, 1983, **219**, 1177.
12 D. J. Cram, *Nature*, 1992, **356**, 29.
13 D. J. Cram and J. M. Cram, *Container Molecules and Their Guests*, (Monographs in Supramolecular Chemistry, No. 4, Series Editor J. F. Stoddart) The Royal Society of Chemistry, Cambridge, U.K. 1997.

14 L. R. MacGillivray and J. L. Atwood, *Angew. Chem., Int. Ed.*, 1999, **38**, 1018.
15 J. Rebek Jr., *Angew. Chem., Int. Ed.*, 2005, **44**, 2068 and references therein.
16 L. C. Palmer and J. Rebek Jr., *Org. Biomol. Chem.*, 2004, **2**, 3051 and references therein.
17 F. Hof, S. L. Craig, C. Nuckolls and J. Rebek, Jr., *Angew. Chem., Int. Ed.*, 2002, **41**, 1488 and references therein.
18 C. H. M. Amijs, G. P. M. van Klink and G. van Koten, *Dalton Trans.*, 2006, 308.
19 M. D. Pluth and K. N. Raymond, *Chem. Soc. Rev.*, 2007, **36**, 161 and references therein.
20 D. Fiedler, D. H. Leung, R. G. Bergman and K. N. Raymond, *Acc. Chem. Res.*, 2005, **38**, 351 and references therein.
21 M. Fujita, M. Tominaga, A. Hori and B. Therrien, *Acc. Chem. Res.*, 2005, **38**, 371.
22 M. Fujita, K. Umemoto, M. Yoshizawa, N. Fujita, T. Kusukawa and K. Biradha, *Chem. Commun.*, 2001, 509.
23 C. L. D. Gibb and B. C. Gibb, *J. Am. Chem. Soc.*, 2004, **126**, 11408.
24 D. H. Leung, R. G. Bergman and K. N. Raymond, *J. Am. Chem. Soc.*, 2006, **128**, 9781 and references therein.
25 D. H. Leung, R. G. Bergman and K. N. Raymond, *J. Am. Chem. Soc.*, 2007, **129**, 2746.
26 M. L. Merlau, M. Del Pilar Mejia, S. T. Nguyen and J. T. Hupp, *Angew. Chem., Int. Ed.*, 2001, **40**, 4239.
27 A. W. Kleij and J. N. H. Reek, *Chem.–Eur. J.*, 2006, **12**, 4218.
28 M. J. Wilkinson, P. W. N. M. van Leeuwen and J. N. H. Reek, *Org. Biomol. Chem.*, 2005, **3**, 2371.
29 M. Kuil, T. Soltner, P. W. N. M. Van Leeuwen and J. N. H. Reek, *J. Am. Chem. Soc.*, 2006, **128**, 11344.
30 A. W. Kleij, M. Lutz, A. L. Spek, P. W. N. M. van Leeuwen and J. N. H. Reek, *Chem. Commun.*, 2005, 3661.
31 V. F. Slagt, P. C. J. Kamer, P. W. N. M. van Leeuwen and J. N. H. Reek, *J. Am. Chem. Soc.*, 2004, **126**, 1526; V. F. Slagt, J. N. H. Reek, P. C. J. Kamer and P. W. N. M. van Leeuwen, *Angew. Chem., Int. Ed.*, 2001, **40**, 4271.
32 T. S. Koblenz, H. L. Dekker, C. G. De Koster, P. W. N. M. Van Leeuwen and J. N. H. Reek, *Chem. Commun.*, 2006, 1700.
33 For an alternative analysis of supramolecular effects in bimolecular reactions using the '*effective molarity*' approach see S. Di Stefano and L. Mandolini, *Acc. Chem. Res.*, 2004, **37**, 113.
34 D. Fiedler, H. van Halbeek, R. G. Bergman and K. N. Raymond, *J. Am. Chem. Soc.*, 2006, **128**, 10240 and references therein.
35 K. Takaoka, M. Kawano, T. Ozeki and M. Fujita, *Chem. Commun.*, 2006, 1625.
36 M. Yoshizawa, M. Tamura and M. Fujita, *Science*, 2006, **312**, 251.
37 A. V. Davis, R. M. Yeh and K. N. Raymond, *Proc. Natl. Acad. Sci. U. S. A.*, 2002, **99**, 4793.
38 J. Kang, J. Santamaria, G. Hilmersson and J. Rebek, Jr., *J. Am. Chem. Soc.*, 1998, **120**, 7389.
39 M. Yoshizawa, T. Kusukawa, M. Fujita, S. Sakamoto and K. Yamaguchi, *J. Am. Chem. Soc.*, 2001, **123**, 10454.
40 J. Chen and J. Rebek, Jr., *Org. Lett.*, 2002, **4**, 327.
41 J. Chen, S. Körner, S. L. Craig, D. M. Rudkevich and J. Rebek, Jr., *Nature*, 2002, **415**, 385.
42 Y. Nishioka, T. Yamaguchi, M. Yoshizawa and M. Fujita, *J. Am. Chem. Soc.*, 2007, **129**, 7000.
43 M. Yoshizawa, Y. Takeyama, T. Kusukawa and M. Fujita, *Angew. Chem., Int. Ed.*, 2002, **41**, 1347.
44 M. Yoshizawa, Y. Takeyama, T. Okano and M. Fujita, *J. Am. Chem. Soc.*, 2003, **125**, 3243.
45 H. Ito, T. Kusukawa and M. Fujita, *Chem. Lett.*, 2000, 598.
46 M. Yoshizawa, S. Miyagi, M. Kawano, K. Ishiguro and M. Fujita, *J. Am. Chem. Soc.*, 2004, **126**, 9172.
47 A. Natarajan, L. S. Kaanumalle, S. Jockusch, C. L. D. Gibb, B. C. Gibb, N. J. Turro and V. Ramamurthy, *J. Am. Chem. Soc.*, 2007, **129**, 4132.
48 A. Greer, *Nature*, 2007, **447**, 273.
49 M. D. Pluth, R. G. Bergman and K. N. Raymond, *Science*, 2007, **316**, 85.

